Proceedings of the ASME 2020
International Mechanical Engineering Congress and Exposition
IMECE2020
November 15-19, 2020, Portland, OR, USA

IMECE2020-23307

VALIDATION OF A PHYSICS BASED THREE PHONON SCATTERING ALGORITHM IMPLEMENTED IN THE STATISTICAL PHONON TRANSPORT MODEL

Michael P. Medlar[1], Edward C. Hensel
Rochester Institute of Technology, Rochester, NY, USA

ABSTRACT

Three phonon scattering is the primary mechanism by which phonon transport is impeded in insulating and semiconducting bulk materials. Accurate computational modeling of this scattering mechanism is required for high fidelity simulations of thermal transport across the ballistic (quantum mechanics) to Fourier (continuum mechanics) range of behavior. Traditional Monte Carlo simulations of phonon transport use a scaling factor such that each scattering event is considered representative of a large number of phonons, often on the order of 10^4 physical phonons per simulated event. The ability to account for every phonon scattering event is desirable to enhance model fidelity. A physics-based model using time dependent perturbation theory (Fermi's Golden Rule) is implemented to compute three phonon scattering rates for each permissible phonon interaction subject to selection rules. The strength of the interaction is based on use of a Gruneisen-like parameter. Both Type I and Type II scattering rates are computed for the allowable interactions that conserve energy and momentum (up to the addition of a reciprocal lattice vector) on a given discretization of momentum space. All of the phonons in the computational domain are represented and phonon populations are updated in momentum space and real space based on the computed number of phonons involved in given scattering events. The computational algorithm is tested in an adiabatic single cell of silicon of dimension 100 x 100 x 100 nm at a nominal temperature of 500 Kelvin containing approximately 10^8 fully anisotropic phonons. The results indicate that phonon populations return to equilibrium if artificially displaced from that condition. Two approaches are introduced to model the relaxation time of phonon states: the single mode relaxation time (SMRT) which is consistent with the underlying assumptions for previously reported theoretical estimates, and the multi model relaxation time (MMRT) which is more consistent with in-situ conditions. The trends meet physical expectations and are comparable to other literature results. In addition, an estimate of error associated with the relaxation times is presented using the statistical nature of the model. The three phonon scattering model presented provides a high fidelity representation of this physical process that improves the computational prediction of anisotropic phonon transport in the statistical phonon transport model.

Keywords: Phonon Transport, Three Phonon Scattering, SPTM

NOMENCLATURE

δ	delta-Dirac function
γ	Gruneisen-like parameter
ψ	state
v_g	group velocity
ω	frequency
Ψ	inter-atomic force constant (~ third derivative)
Π	inter-atomic force constant (~ first derivative)
Φ	inter-atomic force constant (~ second derivative)
a	phonon creation/ annihilation parameter
E	energy
G	reciprocal lattice vector
H	Hamiltonian
i,j,k	unit coordinate directions
k	wave vector
l	lattice vector
M	atomic mass
N	normal modes
n	occupation number
P	probability
s	polarization
u	atomic displacement from equilibrium
V	inter-atomic potential
V	volume

1. INTRODUCTION

Quasi-particle based phonon transport modeling approaches are traditionally called Monte Carlo (MC) simulations. Within these simulations, phonon trajectories are tracked as they undergo various interactions [1]. Accurate

[1] Contact author: mpmmet@rit.edu

representation of scattering interactions is important to produce effective simulations. Scattering is the process by which phonons interact to change their state. Three phonon scattering is the primary process by which phonon transport is impeded in insulating or semiconducting materials. The representation of three phonon scattering in MC simulations been implemented in a variety of ways. Initial works used a constant lifetime [1] or lifetimes in the form of simple phenomenological formulas like those of Klemens [2]. Some only consider the available partners considering conservation of energy and momentum without consideration of a scattering strength parameter [3]. Later enhancements include the use of relaxation times computed from equations proposed by Holland [4]. Relaxation times using Fermi's Golden Rule [5] (time dependent perturbation theory) have been presented in many works like those of Ziman [6], Reissland [7], Srivastava [8], Hans and Klemens [9], Wang and Murthy [10], Esfarjani et al [11], Narumanchi et al [12], Ward and Broido [13], Gutierrez et al [14], Sabatti et al [15], Li et al [16], and others. They have been implemented with varying degrees of sophistication. Relative to the models associated with the MC approach, they typically lack in several areas. The scattering algorithms all rely on random number generation and do not typically directly result in conservation of energy and momentum. For example, Wu et al [17] implements a technique that is common in the MC simulation where scattered phonons are deleted from the simulation domain and new ones are introduced randomly from the equilibrium distribution. The actual number of phonons involved in scattering are not physically distributed among the partner states. This does not result in conservation of momentum or energy in an individual scattering event. All use scaling factors to represent the actual number of phonons in a given volume and in scattering events. For example, Sabatti et al. [18] simulated phonon transport in a 2 μm silicon thermal resistor at 300 K using 130,000 particles where each nanosecond of simulation required 1h and 30 minutes of wall clock time on 50 core processors (the type was not specified). With a cross section of 50 nm, there are on the order of 10^8 phonons in this domain. Thus, only representing a little over 0.1% of the phonons in the domain. Kukita et al. [19-21] simulated phonon transport in FinFETs with a gate length of 22 nm and Fin thickness of 8 nm utilizing about 10,000 particles. The Statistical Phonon Transport Model (SPTM) [22-24] was introduced to overcome some of the deficiencies of the physical models and algorithms of traditional MC codes. It is based on algorithms that allow for representation of all of the phonons in a given geometric domain, to eliminate use of scaling factors. Within three phonon scattering, energy and momentum conservation is strictly enforced. The need for random number generation is eliminated because all of the phonons of a given type are distributed according to the probability of a given interaction, computed from basic physical principles, among all partner states. Thus, the SPTM allows for increased physicality and higher fidelity phonon transport modeling compared to MC. In addition, it is well suited for increased computational efficiency as individual phonon trajectories are not tracked and the code was developed to be implemented in a parallel nature. The SPTM can be a flexible, efficient, and accurate tool for device level phonon transport modeling applications. It will allow engineers to solve significant problems of practical importance in the area of thermal energy management in nanoscale devices.

2. METHODS

2.1 Theory

Phonons involve vibrational excitations of the atomic lattice. Three phonon scattering creates an interaction that changes this state. The probability that the vibrational state changes with time due to three phonon scattering can be predicted with time dependent perturbation theory using Fermi's Golden Rule [5] shown in equation 1,

$$\dot{P}_{n-m} \cong \frac{2\pi}{\hbar} |\langle \psi_m | H'(t) | \psi_n \rangle|^2 \delta(E_n - E_m)\,, \tag{1}$$

where $\dot{P}_{n-m}$ is the probability of transition from state n to m as a function of time, $\langle \psi_m | \mathrm{H}'(\mathrm{t}) | \psi_n \rangle$ is referred to as the matrix element, or transition amplitude, as it connects the states ψ_n and ψ_m through the perturbation $H'(t)$, and $\delta(\mathrm{E_n} - \mathrm{E_m})$ is a delta function that enforces energy conservation. Application of Fermi's Golden Rule to the three phonon interaction involves some modification. The initial state is represented as the state where three phonons are present and the final state is one in which the population of the reactions either decreases or increases based on the type of event. These states are shown with equations 2 – 4 [25].

$$|\psi_n\rangle = |\, n_{ks}, n_{k's'}, n_{k"s"}\rangle \tag{2}$$

$$|\psi_m\rangle_{Type\ I} = |\, n_{ks} - 1, n_{k's'} - 1, n_{k"s"} + 1\rangle \tag{3}$$

$$|\psi_m\rangle_{Type\ II} = |\, n_{ks} + 1, n_{k's'} + 1, n_{k"s"} - 1\rangle \tag{4}$$

The states are identified with the occupation number, n and are labeled by the individual phonon wavevector $(\mathrm{k}, \mathrm{k}', \mathrm{k}")$ and polarization $(\mathrm{s}, \mathrm{s}', \mathrm{s}")$. In addition to specifying the initial and final states, the perturbing Hamiltonian must be specified for use in Fermi's Golden Rule. For the three phonon interaction this is the deviation in the interatomic potential from harmonic. Typically, the interatomic potential is expressed as a Taylor series expansion about the equilibrium position of the atoms. This can be expressed as equation 5 [11],

$$V = V_o + \sum_i \Pi_i u_i + \frac{1}{2!}\sum_{ij} \Phi_{ij} u_i u_j + \frac{1}{3!}\sum_{ijk} \Psi_{ijk} u_i u_j u_k + \cdots \tag{5}$$

where $\mathrm{u_i}$ is the displacement of the atom at location i about its equilibrium position and, Π_i, Φ_ij, Ψ_ijk are known as the interatomic force constants. They are related to the first, second, and third derivative of the interatomic potential respectively. We are interested in only the third order term for the perturbing Hamiltonian. The classical expression for this is shown with equation 6 [8]:

$$H'(t) = \frac{1}{3!}\sum_{ijk} \Psi_{ijk} u_i u_j u_k \tag{6}$$

Specification of the perturbing Hamiltonian in a form appropriate for use in Fermi's Golden Rule involves promotion of the displacement variables to quantum mechanical operators. This is defined in equation 7 [7],

$$u_{lx} = \frac{1}{\sqrt{N}} \sum_{ks} \left(\frac{\hbar}{2M\omega(k)} \right)^{1/2} \left(a_{ks}^{\dagger} - a_{ks} \right) e^{-i\mathbf{k}\cdot\mathbf{l}} \tag{7}$$

where M is the atomic mass, N is the number of normal modes over which the summation is performed, ω(k) is the frequency associated with phonon mode k, $a_{ks}^{\dagger}$ is the phonon creation operator that creates of phonon of wavevector k and polarization s, a_{ks} is the phonon annihilation operator that destroys a phonon with wavevector k and polarization s and l is a lattice vector. Substituting the definition of the displacement operator from equation 7, it can be shown [7] that the perturbing Hamiltonian of equation 6 becomes equation 8.

$$H'(t) = \sum_{l\, l'} \sum_{l"} \sum_{kk'k''} \frac{1}{3!} \left(\frac{\hbar^3}{8M^3N^3\omega(k)\omega\prime(k\prime)\omega"(k")} \right)^{\frac{1}{2}} \Psi_{ijk} \left(a_{ks}^{\dagger} - a_{ks} \right) \left(a_{k\prime s}^{\dagger} - a_{k\prime s} \right) \left(a_{k"s}^{\dagger} - a_{k"s} \right) e^{i\mathbf{k}\cdot\mathbf{l}} e^{i\mathbf{k}'\cdot\mathbf{l}\prime} e^{i\mathbf{k}''\cdot\mathbf{l}"} \tag{8}$$

Equation 8 involves summations over the three wavevectors of phonons involved in addition to the locations of the three adjacent atoms of the lattice (labeled by lattice vectors to their locations l, l', and l"). This can be further simplified by considering that the above expression should be invariant under translation. That is, if we add a lattice vector (move to a different spot in the crystal) the results should be unchanged. Thus, if we add a lattice vector l to each one of the lattice vectors l, l' and l" the following term is introduced:

$$\frac{1}{N} \sum_{l} e^{i(\mathbf{k}+\mathbf{k}'+\mathbf{k}")\cdot l} \tag{9}$$

This expression is zero unless $\mathbf{k} + \mathbf{k}' + \mathbf{k}"$ is equal to zero or a reciprocal lattice vector (G). This amounts to a delta function that has the effect of conserving momentum. In addition, we can take the origin of our lattice to be at position l. Equation 8 is them simplified to equation 10.

$$H'(t) = \sum_{l\, l'} \sum_{l"} \sum_{kk'k''} \frac{1}{3!} \left(\frac{\hbar^3}{8M^3N\omega(k)\omega\prime(k\prime)\omega"(k")} \right)^{1/2} \Psi_{ijk} \left(a_{ks}^{\dagger} - a_{ks} \right) \left(a_{k\prime s}^{\dagger} - a_{k\prime s} \right) \left(a_{k"s}^{\dagger} - a_{k"s} \right) e^{i\mathbf{k}'\cdot\mathbf{l}\prime} e^{i\mathbf{k}''\cdot\mathbf{l}"} \delta_{k+k'+k''+G} \tag{10}$$

Substituting into Fermi's Golden Rule (equation 1) for a Type I interaction, equation 11 results.

$$\dot{P}_{n-m} \cong \frac{2\pi}{\hbar} \left| \langle \psi_m(x) | \sum_{l\, l'} \sum_{l"} \sum_{kk'k''} \frac{1}{3!} \left(\frac{\hbar^3}{8M^3N\omega(k)\omega\prime(k\prime)\omega"(k")} \right)^{\frac{1}{2}} \Psi_{ijk} \left(a_{ks}^{\dagger} - a_{ks} \right) \left(a_{k\prime s}^{\dagger} - a_{k\prime s} \right) \left(a_{k"s}^{\dagger} - a_{k"s} \right) e^{i\mathbf{k}\cdot\mathbf{l}} e^{i\mathbf{k}'\cdot\mathbf{l}\prime} e^{i\mathbf{k}''\cdot\mathbf{l}"} \delta_{k+k'+k''+G} \, |\psi_n(x)\rangle \right|^2 \delta(E_n - E_m) \tag{11}$$

A slight simplification produces equation 12.

$$\dot{P}_{n-m} = \frac{2\pi}{\hbar} \left\{ \sum_{l\, l'} \sum_{l"} \sum_{kk'k''} \frac{1}{3!} \left(\frac{\hbar^3}{8M^3N\omega(k)\omega\prime(k\prime)\omega"(k")} \right)^{\frac{1}{2}} \Psi_{ijk} e^{i\mathbf{k}\cdot\mathbf{l}} e^{i\mathbf{k}'\cdot\mathbf{l}\prime} e^{i\mathbf{k}''\cdot\mathbf{l}"} \delta_k \, \delta_E \right\}^2 \cdot \left| \langle \psi_m(x) | \left(a_{ks}^{\dagger} - a_{ks} \right) \left(a_{k's}^{\dagger} - a_{k's} \right) \left(a_{k"s}^{\dagger} - a_{k"s} \right) | \psi_n(x) \rangle \right|^2 \tag{12}$$

Evaluation of the squared modulus requires knowledge of how the annihilation and creation operators act on the three phonon state. This is shown with equations 13 – 14.

$$a_{ks}^{\dagger} | \, n_{ks}, n_{k\prime s\prime}, n_{k"s"} \rangle = (n_{ks} + 1)^{1/2} | \, n_{ks} + 1, n_{k\prime s\prime}, n_{k"s"} \rangle \tag{13}$$

$$a_{ks} | \, n_{ks}, n_{k's'}, n_{k"s"} \rangle = (n_{ks})^{1/2} | \, n_{ks} - 1, n_{k's'}, n_{k"s"} \rangle \tag{14}$$

Enforcing orthogonality of the state vectors implies that the only terms that will survive the inner product are the ones where the groups of three operators act on the initial state to produce the final state. For a Type I event, there are only six terms in the summation over the wavevectors (k, k' and k") that result in a non-zero inner product. They also all produce the same value and an example of this for a Type I event is shown in equation 15 [26].

$$\begin{aligned} &\langle \, n_{ks} - 1, n_{k's'} - 1, n_{k"s"} + 1 | a_{ks} a_{k's'} a_{k"s"}^{\dagger} | \, n_{ks}, n_{k\prime s\prime}, n_{k"s"} \rangle \\ &= \langle \, n_{ks} - 1, n_{k's'} - 1, n_{k"s"} + 1 | \, (n_{ks})^{\frac{1}{2}} \, (n_{k's'})^{\frac{1}{2}} \, (\, n_{k"s"} + 1)^{\frac{1}{2}} \, | \, n_{ks} - 1, n_{k's'} - 1, n_{k"s"} + 1 \rangle \\ &= \, (n_{ks})^{\frac{1}{2}} \, (n_{k's'})^{\frac{1}{2}} (\, n_{k"s"} + 1)^{\frac{1}{2}} \langle \, n_{ks} - 1, n_{k's'} - 1, n_{k"s"} + 1 || \, n_{ks} - 1, n_{k's'} - 1, n_{k"s"} + 1 \rangle \\ &= \, (n_{ks})^{\frac{1}{2}} \, (n_{k's'})^{\frac{1}{2}} (\, n_{k"s"} + 1)^{\frac{1}{2}} \end{aligned} \tag{15}$$

The transition rate for a Type I scattering event becomes equation 16.

$$\dot{P}_{n-m} \cong \frac{\pi}{\hbar} \frac{1}{3!^2} \frac{\hbar^2}{4M^3N\omega(k)\omega'(k')\omega"(k")} \cdot \sum_{l} \left(\Psi_{ijk} e^{i\mathbf{k}\cdot\mathbf{l}} e^{i\mathbf{k}'\cdot\mathbf{l}'} e^{i\mathbf{k}''\cdot\mathbf{l}"} \right)^2 n_{ks} n_{k's'} (n_{k"s"} + 1) \, \delta(\omega(\mathrm{k}) - \omega'(k') - \omega"(k")) \tag{16}$$

Prior to implementation of the above equation, the anharmonic strength term (the Fourier transform of the third order derivative of the interatomic potential) must be specified. This work approximates the term $\Psi_{ijk}e^{i\mathbf{k}\cdot\mathbf{l}}e^{i\mathbf{k}'\cdot\mathbf{l}'}e^{i\mathbf{k}''\cdot\mathbf{l}''}$ using the Gruneisen parameter [11], as shown in equation 17,

$$\sum_l \Psi_{ijk} e^{i\boldsymbol{k}\cdot\boldsymbol{l}} e^{i\boldsymbol{k}'\cdot\boldsymbol{l}'} e^{i\boldsymbol{k}''\cdot\boldsymbol{l}''} \cong \frac{-6\gamma_{ks}M\omega"(k")^2}{a}\ , \qquad (17)$$

where γ_{ks} is the Gruneisen parameter, M is the atomic mass, $\omega"(k")$ is the frequency of the third phonon partner and a is the lattice constant. The Gruneisen parameter is directly related to the change in normal mode frequency due to a change in the lattice constant of the crystal thus, it is physically reasonable to use this parameter to estimate the anharmonic scattering strength as it is directly related to the anharmonic nature of the interatomic potential. (The Gruneisen parameter is treated as an adjustable parameter that is modified to reproduce physically expected results at Fourier length scales when the three phonon scattering model is incorporated into the SPTM. This will help ensure physically accurate representation of this scattering mechanism.) The transition rate for a Type I interaction becomes equation 18.

$$\dot{P}_{n-m} \cong \frac{\pi\hbar}{4M^3N\omega(k)\omega\prime(k\prime)\omega"(k")}\left(\frac{\gamma_{ks}^2M^2\omega"(k")^4}{a^2}\right)n_{ks}n_{k's'}(n_{k"s"}+1)\delta(\omega(\mathrm{k})-\omega'(k')-\omega"(k")) \quad (18)$$

The SPT Model of Brown III and Hensel [22] computes an interaction table for use in three phonon scattering implementation. This interaction table consists of pseudo-states that can participate in three phonon scattering events based on the selection rules for energy and momentum conservation. Each pseudo-state represents a volume in wavevector space. For a given scattering interaction, the scattering rate must be modified to represent this fact. As in the form of equation 18, it can be thought of as the scattering rate per unit volume in real space and in wave vector space. This amounts to the following manipulation.

$$\dot{P}_{n-m} \cong \frac{\pi\hbar}{4M^3N\omega(k)\omega\prime(k\prime)\omega"(k")}\left(\frac{\gamma_{ks}^2M^2\omega"(k")^4}{a^2}\right)n_{ks}n_{k\prime s\prime}(n_{k"s"}+1)\sum_{k-volume}\delta(\omega(\mathrm{k})-\omega'(k')-\omega"(k")) \qquad (19)$$

The summation can be transformed to an integral in wavevector space as in equation 20.

$$\dot{P}_{n-m} \cong \frac{\pi\hbar}{4M^3N\omega(k)\omega\prime(k\prime)\omega"(k")}\left(\frac{\gamma_{ks}^2M^2\omega"(k")^4}{a^2}\right)n_{ks}n_{k\prime s\prime}(n_{k"s"}+1)\int\frac{V}{(2\pi)^3}\delta(\omega(\mathrm{k})-\omega'(k')-\omega"(k"))d\boldsymbol{k} \qquad (20)$$

The integral of the delta function over the region in wavevector space can be changed to an integral over a surface in wavevector space where the frequency is within an infinitesimal band and thus energy conservation is satisfied. The following substitution (equation 21) can be made [27],

$$\int_k \frac{V}{(2\pi)^3}\delta(\omega(\mathrm{k})-\omega'(k')-\omega"(k"))d\boldsymbol{k} = \int_\omega \frac{V}{(2\pi)^3}\delta(\omega(\mathrm{k})-\omega'(k')-\omega"(k"))\frac{dSdkd\omega}{d\omega}\ , \qquad (21)$$

where, V is the volume of the crystal, $\frac{d\omega}{dk}$ is the group velocity (v_g) and S is a surface in momentum space of constant wavevector. The integral of the delta function with respect to frequency becomes unity and equation 20 becomes equation 22.

$$\dot{P}_{n-m} \cong \frac{\pi\hbar}{4M^3N\omega(k)\omega\prime(k\prime)\omega"(k")}\left(\frac{\gamma_{ks}^2M^2\omega"(k")^4}{a^2}\right)n_{ks}n_{k\prime s\prime}(n_{k"s"}+1)\frac{V}{(2\pi)^3}\int_{k-cel}\frac{dS}{v_g} \qquad (22)$$

The remaining difficulty comes in evaluating the integral over the surface S. It is assumed the surface takes a spherical shape. Thus, the integral results in a portion of the surface area of a sphere that is contained within one of the volume elements in k-space. This surface area is approximated as the cross sectional area of a pseudo-state volume element ($\Delta k_x \Delta k_y$).

2.2 Implementation.

Application of the scattering rate model from Fermi's Golden Rule to calculate three phonon scattering within the framework of the statistical phonon transport model begins with computation of the available scattering partners within the geometric domain and the phase space that ensure both energy and momentum conservation. This is done through the creation of an interaction table that is pre-computed and stored for scattering calculations [22-24]. This concept is similar to, but predates, that of Sabatti et al [18]. Computation of the interaction table starts with a search scheme applied to the discretized First Brillouin Zone (FBZ). In this initial step, the wavevector of the centroid of each element is compared to every other one in the FBZ to determine all of the combinations that conserve momentum. Because phonons are assumed to be evenly distributed over the k-space element, the size of the volume element must be considered when applying momentum conservation constraints. That is, it is possible for phonons that are relatively low in wavevector within each combination to produce phonons outside of the resultant element if just centroids are considered. This is accounted for in the fact that each combination of two element partners can add to create one of eight possible outcomes. This is illustrated in a two dimensional case with Figure 1,

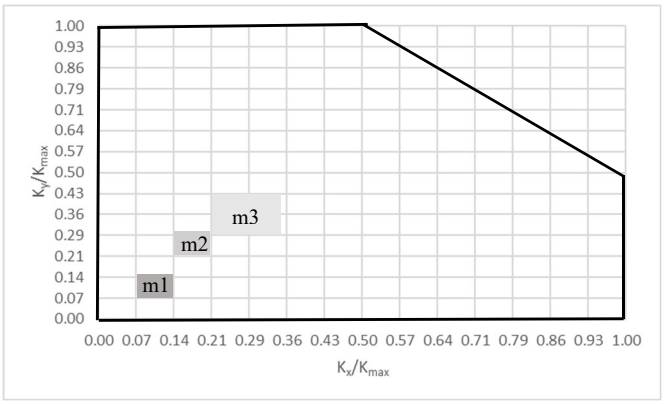

FIGURE 1: DETERMINATION OF INTERACTING ELEMENTS. REPRODUCED FROM [22].

where m1 and m2 indicate the two scattering partner elements that combine to produce element m3. Momentum conservation is ensured up to the addition of a reciprocal lattice vector (G) and both normal and Umklapp processes are considered.

If an interaction is deemed to satisfy momentum conservation, it is then checked for energy conservation. This is done by comparing the frequencies of each of the six modes at the centroid of a given element to the frequencies of the modes corresponding to the centroids of the partner elements. Comparison of the frequencies to satisfy energy conservation involves the use of a pre-specified relative tolerance (ω_{eps}). This is illustrated with equation 23.

$$\frac{\omega^{"}(k^{"})-\omega'(k')-\omega(k)}{\omega^{"}(k^{"})} < \omega_{eps} \tag{23}$$

The interactions that are deemed to meet the criteria of equation 23 are included in the three phonon scattering interactions. The number of interactions that result is directly dependent on the value of the tolerance. Too small of a tolerance will result in artificially limiting the number of interactions. And conversely, too large of a tolerance will allow too many interactions that will be both computationally intensive and induce non-physical results. Based on a sensitivity performed, this work selected a tolerance that was large enough to ensure that all pseudo-states within the FBZ are ensured to have at least one scattering interaction. Thus, there are zero non-participating states. This ensures that the change in the population (number of phonons) of a given pseudo-state will have a basis in the three phonon scattering physics discussed in the preceding section. The value used for the tolerance that meets this criteria is 2.75 E-5, which is approximately five orders of magnitude less than the value of $\omega^{"}(k^{"})$. If a three phonon partner passes the energy and momentum checks, it is added to the interaction table and the process continues. The current work uses a table that involves 1,334,112 three phonon scattering interactions. The value of the tolerance, ω_{eps}, is dependent on the mesh size chosen to discretize the FBZ. At larger mesh values, the size of the volume element in wavevector (and therefore frequency) space will be smaller. This has the effect of enforcing a tighter tolerance on energy conservation and implies that the value of ω_{eps} could also be reduced to produce the same effect noted above in regard to ensuring all pseudo-states have at least one scattering interaction.

After computation of the available three phonon scattering partners, scattering is computed at each computational time step within the geometric domain of interest. A value of 1 ps was used for the time step and the size of the geometric domain was a 100 nm cube. In general, the size of the geometric cell is chosen such that no single phonon can traverse a single cell in a single time step. Thus, all phonons within the geometric cell are assumed to have the ability to participate in three phonon scattering. The equations for the scattering rates (Type I Rate and Type II Rate) computed from Fermi's Golden Rule (equation 22) are applied to each interaction listed in the interaction table. This allows for the computation of a probability of both a Type I and Type II interaction in the chosen time step. This probability is applied to the population of phonons associated with the least populated state involved in the interaction to compute the number of Phonons Created or Phonons Destroyed due to the single scattering event in a single time step. An illustration of the results of this calculation applied to three, three phonon interactions is shown in Table 1,

TABLE 1: EXAMPLE OF IMPLEMENTATION OF SCATTERING EQUATIONS IN INTERACTION TABLE

Partner 1			Partner 2			Partner 3			Type I Rate	Type II Rate	Phonons Created	Phonons Destroyed
k	ω	n	k'	ω'	n'	k"	ω"	n"				
(1/m)	(rad/s)	(-)	(1/m)	(rad/s)	(-)	(1/m)	(rad/s)	(-)	(1/s)	(1/s)	(#)	(#)
7.16E+08	2.50E+12	25.6862	6.33E+09	2.12E+13	2.61457	7.43E+09	2.37E+13	2.29203	9.25E+09	9.25E+09	4.82E+01	4.82E+01
1.37E+09	4.86E+12	12.9749	6.55E+09	8.67E+13	0.362271	6.95E+09	9.15E+13	0.328244	5.23E+09	5.24E+09	3.93E+00	3.94E+00
2.95E+09	2.38E+13	2.28055	1.09E+10	6.46E+13	0.594211	1.21E+10	8.84E+13	0.349733	7.15E+08	7.15E+08	5.69E-01	5.69E-01

where the wavevector (k), frequency (ω), and occupation number of phonons (n) are shown for each of the three scattering partners involved in a given interaction. All energy and momentum conserving events in the interaction table involving a given pseudo-state are considered when determining the overall change in the population of that state. Thus, populations

are updated with exact number of phonons created or destroyed and this redistribution of phonons from scattering is done within the phase space.

3. RESULTS AND DISCUSSION

Implementation of the scattering algorithm described within the framework of the SPTM leads to physically accurate results and allows for physical insight not attainable with other methods.

The scattering algorithm returns the phonon population to the Bose Einstein equilibrium [27] distribution after being initially displaced from that condition at a rate which is physically reasonable and comparable to prior results in literature. This is first illustrated by displacing single states from equilibrium (one at a time) and allowing them to decay back to equilibrium.
The rate at which a select state decays to equilibrium is shown with Figure 2.

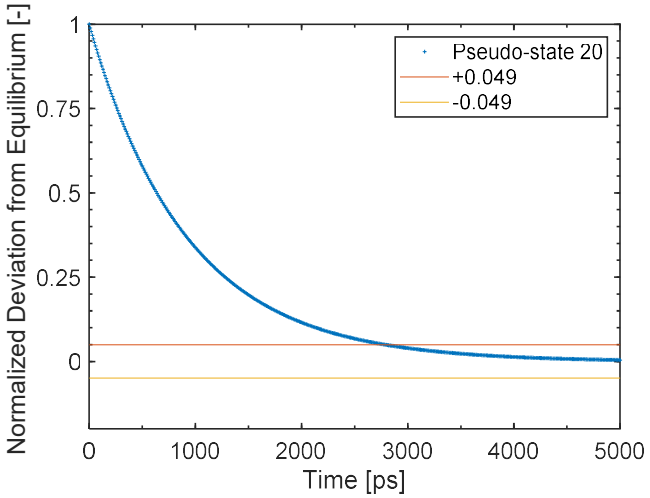

FIGURE 2: NORMALIZED SINGLE MODE PHONON POPULATION DECAY FOR PSEUDO-STATE 20 DUE TO THREE PHONON SCATTERING

Since all other states are at equilibrium in this scattering simulation, this is representative of the single mode decay rate. Typically, phonon state dynamics are illustrated with the single mode relaxation time (SMRT) concept. The SMRT is defined as the representative time over which a given state decays to equilibrium if it is the only state perturbed from equilibrium. It is illustrated with equation 24 [28],

$$-\frac{\partial n_{ks}}{\partial t}\Big|_{scattering} = \frac{n_{ks}-\bar{n}_{ks}}{\tau_{ks}} \quad (24)$$

where n_{ks} is the time dependent phonon distribution function, $\bar{n}_{ks}$ is the Bose Einstein distribution function and τ_{ks} is the relaxation time associate with the mode ks. The SMRT concept inherently assumes that the decay curve is exponential in nature and this is not always a good fit. This work presents results which may be compared to reported values of SMRT by estimating a single mode decay time constant. The time when the population of a given mode has decayed to within 4.98 percent of equilibrium is defined equal to three time constants. For pseudo-state 20 (Figure 3), this definition produces an estimated SMRT of 2810/3 ps or 937 ps. The scattering algorithm presented herein was used to estimate SMRT values for acoustic and optical modes in the 100 direction in Figure 4.

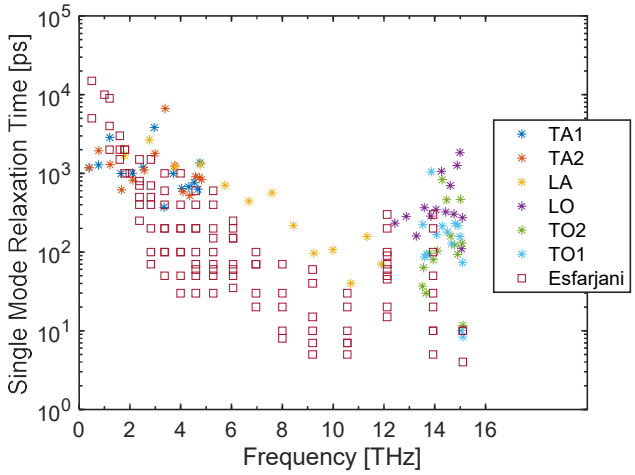

FIGURE 3: SINGLE MODE RELAXATION TIMES. PREDICTIONS IN 100 DIRECTION, MESH 14, GUNEISEN OF 1.1 AND T= 500K. NOTE THAT THE DATA FROM ESFARJANI [11] IS FOR ALL DIRECTIONS AND AT 277K.

Figure 3 compares the values computed from this work to those of Esfarjani et al. [11]. The general range of values and trends agree. It is noted that this is not precisely a 1:1 comparison, as the Esfarjani data is for all directions and differs in temperature from those of this work. As future work, a comparison of SMRT's will be made at the same temperature and the Gruneisen parameter will be used as an adjustable input to ensure that the SPTM can reproduce higher fidelity published relaxation times as well as physically expected thermal conductivities at Fourier length scales. This may seem arbitrary but it is no more arbitrary than the choice of an energy conservation tolerance as this directly affects the number of allowed scattering interactions and thus the relaxation times of a given pseudostate.

Single mode decay is not a physically realistic scenario and is a concept which has been previously introduced as the result of prior numerical algorithm approximations. A transient that would tend to perturb one state from equilibrium will likely perturb other state from equilibrium in a physical setting. To simulate this effect, the phonon distribution is randomly displaced from equilibrium by at most either positive thirty-five percent or negative thirty-five percent. The scattering algorithm is then implemented, and the phonon population is allowed to relax due to three phonon interactions back to equilibrium. The initially perturbed phonon population is shown relative to equilibrium in Figure 4,

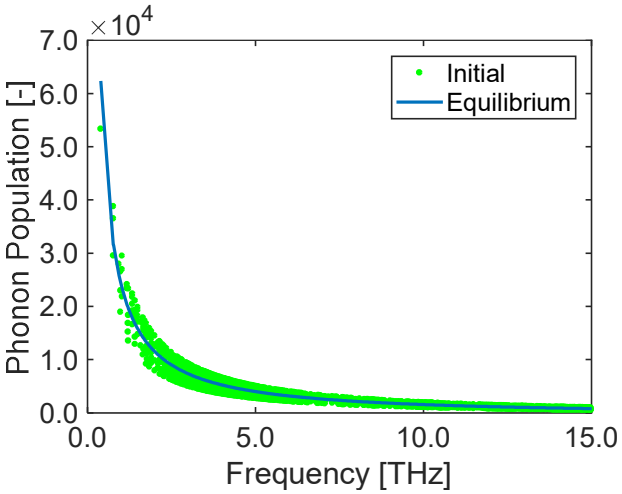

FIGURE 4: INITIAL PHONON POPULATION FOR SCATTERING TESTING RELATIVE TO EQUILIBRIUM. ISOTHERMAL 100 NM CELL AT A TEMPERATURE OF 500 K.

where the solid blue line represents the equilibrium number of phonons expected in a 100 nm cell of silicon at 500 K as a function of frequency in THz. The solid green circles show the artificially displaced phonon population at time zero. As the calculation proceeds over a given amount of time, the relaxation of the population to equilibrium is shown with Figure 5.

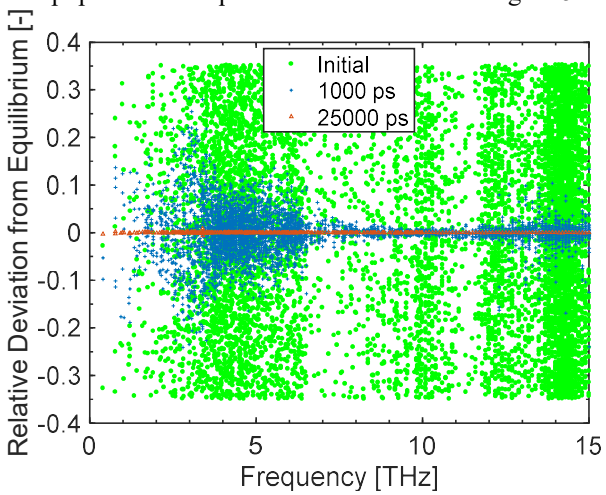

FIGURE 5: RELATIVE DEVIATION OF THE PHONON POPULATION FROM EQUILIBRIUM

The solid green circles are the initial phonon population, the blue plus signs indicate the relative deviation after 1000 ps and the red triangles after 25 000 ps. The results demonstrate that, absent external influences, the phonon population tends toward equilibrium. This is physically reasonable behavior and expected from the formulation of the scattering algorithm.

The results from Figure 5 show the overall phonon population dynamics but, it is also of interest to examine individual pseudo-state dynamics. This can be shown with the specific phonon populations as a function of time for a select number of pseudo-states. The relaxation of the six modes corresponding to a given wavevector are considered in Figure 6. This relaxation rate is referred to as the Multi-mode relaxation time (MMRT) to distinguish it from the SMRT.

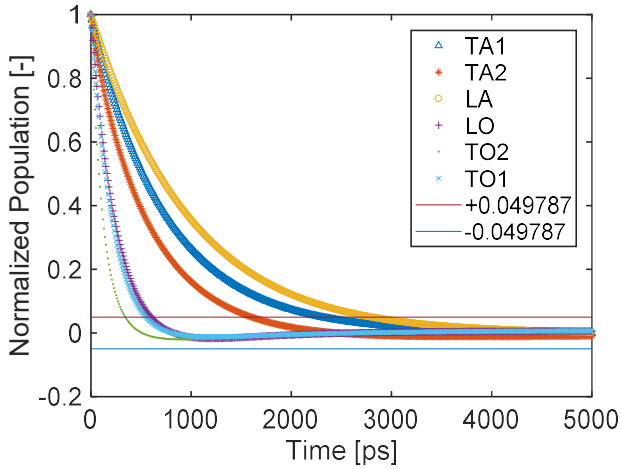

FIGURE 6: NORMALIZED PHONON POPULATION DECAY DUE TO SCATTERING FOR SIX MODES AT A WAVEVECTOR OF 3.76E9 1/M. THE FREQUENCIES RANGE FROM APPROXIMATELY 2 THZ FOR TA1 TO 14.9 THZ FOR TO1.

The different markers illustrate the decay curves of the acoustic and optical modes at a wavevector of 3.76E9 1/m in the 100 direction. All curves show the normalized deviation in the phonon population from equilibrium as a function of time. As each curve represents a different phonon mode at a given wave vector, they are all at different frequencies. In general, the higher frequency optical modes have smaller MMRT than the relatively lower frequency acoustic modes. This is due to the fact that the scattering strength is directly related to the frequency of the mode as well as the fact that the higher frequency modes have a larger number of scattering partners as they can decay into many different combinations of pseudo-states.

The flexibility of the scattering algorithm in the SPTM and the physical nature of the model itself allows investigation into phenomenon that may not be available in other models and confidence in associated predictions. One such phenomenon is the sensitivity of the MMRT to the initial deviation and condition of partner pseudo-states from equilibrium. The symmetry of the FBZ in the SPTM and the random nature of the initial condition allows this to be determined with relative ease as multiple samples of decay from a given pseudo-state are available within a given simulation. This is shown with Figure 7,

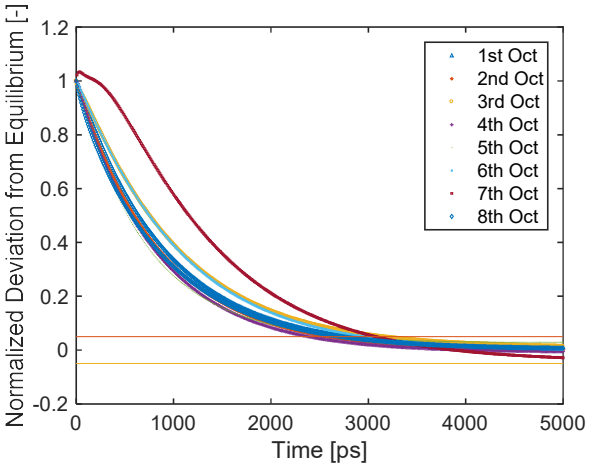

FIGURE 7: NORMALIZED POPULATION DECAY FOR THE EIGHT REPLICATES OF A GIVEN PSEUDO-STATE. LA, 100 DIRECTION, $\omega = 3.7879$ THZ.

where each curve indicates decay of a pseudo-state represented in the SPTM. Each of the pseudo-states illustrated above have the same characteristics (wavevector, frequency, and population) because of symmetry of the FBZ. The three phonon partner states associated with the above pseudo-states share the same characteristics of wavevector and frequency. They differ only in the relative deviation of those states from equilibrium due to the random initial condition. One may postulate that the random nature of the displacement from equilibrium would produce a net zero effect on the scattering rates. This is not the case as all interactions are not equally weighted in regard to the overall effect on the population of a given state. Some have a larger affect due to the characteristics of the interacting phonons. The occupancy of the partner states has a direct effect on the computed scattering rates for a given interaction and thus has a direct effect on the relaxation of the state to equilibrium despite all other factors being equal. That is, the rate of decay of any given state to equilibrium is directly affected by the state of the entire system. This leads to variability in the relaxation time. This variability is shown for all the longitudinal acoustic pseudo-states in the 100 direction with Figure 8.

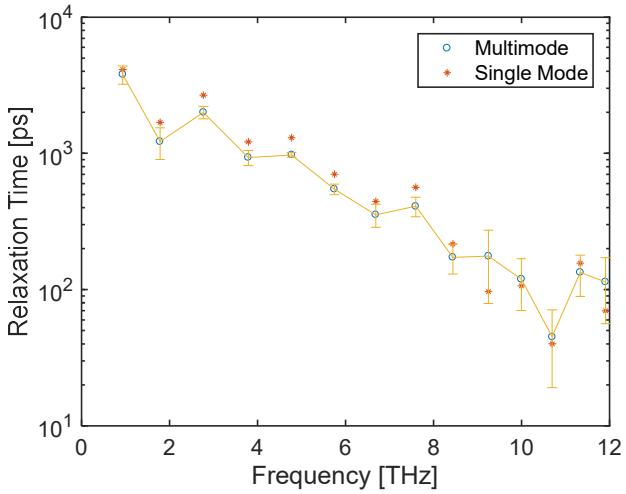

FIGURE 8: LONGITUDINAL ACOUSTIC MMRT WITH ERROR BARS COMPARED TO SMRT. 100 DIRECTION, GUNEISEN OF 1.1, AND T= 500K.

Figure 9 shows the average multi-mode relaxation time for the LA states in the 100-direction computed from decay rates of the eight symmetric states in the FBZ. It demonstrates that significant variability in the MMRT can occur due to the exact configuration of all partner pseudo-states.

4. CONCLUSION

A physics based three phonon scattering algorithm employing Fermi's golden rule to approximate the probability of discrete phonon interactions has been presented within the framework of the Statistical Phonon Transport Model (SPTM). The algorithm enforces strict conservation of energy and momentum in contrast to traditional Monte Carlo algorithms. Results demonstrate the algorithm achieves full fidelity of the entire phonon population present in a physical domain, while incorporating fully anisotropic dispersion relations and permitted all concurrent phonon polarizations. Results demonstrate the algorithm approaches the theoretical limit of the Bose distribution when arbitrarily disturbed from equilibrium. Results from the scattering algorithm exhibit good agreement with previously published reports of the Single Mode Relaxation Time (SMRT). The Multi-Mode Relaxation Time (MMRT) is a measure of phonon relaxation time which better reflects physical phenomena occurring in crystalline lattice materials. The physically realistic theory underlying the scattering algorithm, in conjunction with the numerical framework of the SPTM, will allow flexible, efficient, and accurate prediction of thermal behavior in nanoscale devices over a range of length and time scales.

ACKNOWLEDGEMENTS

The authors would like to acknowledge useful e-mail communications from Dr. Kevian Esfarjani.

REFERENCES

[1] Peterson, R. B., 1994, "Direct Simulation of Phonon-Mediated Heat-Transfer in a Debye Crystal," JOURNAL OF HEAT TRANSFER-TRANSACTIONS OF THE ASME, 116(4), pp. 815-822.
[2] Klemens, P. G., 1958, Elsevier Science & Technology.
[3] Mazumder, S., and Majumdar, A., 2001, "Monte Carlo Study of Phonon Transport in Solid Thin Films Including Dispersion and Polarization," JOURNAL OF HEAT TRANSFER-TRANSACTIONS OF THE ASME, 123(4), pp. 749-759.
[4] Holland, M. G., 1963, "Analysis of Lattice Thermal Conductivity," Physical Review, 132(6), pp. 2461-2471.
[5] Sakurai, J. J., and Napolitano, J., 2011, Modern Quantum Mechanics, Addison-Wesley, Boston.
[6] Ziman, J. M., 1960, Electrons and Phonons, Oxford, Great Britain.
[7] Reissland, J. A., 1973, The Physics of Phonons, Wiley, London;New York;.
[8] Srivastava, G. P., The Physics of Phonons.
[9] Han, Y., and Klemens, P. G., 1993, "Anharmonic Thermal Resistivity of Dielectric Crystals at Low Temperatures," Physical review. B, Condensed matter, 48(9), pp. 6033-6042.
[10] Wang, T., and Murthy, J. Y., 2006, "Solution of the Phonon Boltzmann Transport Equation Employing Rigorous Implementation of Phonon Conservation Rules," Proc. ASME International Mechanical Engineering Congress and Exposition, Chicago, Illinois, USA.
[11] Esfarjani, K., Chen, G., and Stokes, H. T., 2011, "Heat Transport in Silicon from First-Principles Calculations," Physical Review B, pp. 11.
[12] Narumanchi, S. V. J., Murthy, J. Y., and Amon, C. H., 2004, "Submicron Heat Transport Model in Silicon Accounting for Phonon Dispersion and Polarization," Journal of Heat Transfer, 126(6), pp. 946.
[13] Ward, A., and Broido, D. A., 2010, "Intrinsic Phonon Relaxation Times from First-Principles Studies of the Thermal Conductivities of Si and Ge," Physical Review B.
[14] Pascual-Gutiérrez, J. A., Murthy, J. Y., and Viskonta, R., 2009, "Thermal Conductivity and Phonon Transport Properties of Silicon Using Perturbation," Journal of Applied Physics 106.
[15] Sabatti, F. F. M., Goodnick, S. M., and Saraniti, M., 2016, "Simulation of Phonon Transport in Semiconductors Using a Population Dependent Many-Body Cellular Monte Carlo Approach," Journal of Heat Transfer.
[16] Li, W., Carrete, J., A. Katcho, N., and Mingo, N., 2014, "Shengbte: A Solver of the Boltzmann Transport Equation for Phonons," Computer Physics Communications, 185(6), pp. 1747-1758.
[17] Wu, R., Hu, R., and Luo, X., 2016, "First-Principle-Based Full-Dispersion Monte Carlo Simulation of the Anisotropic Phonon Transport in the Wurtzite Gan Thin Film," Journal of Applied Physics, 119(14), pp. 145706.
[18] Sabatti, F. F. M., Goodnick, S. M., and Saraniti, M., 2017, "Simulation of Phonon Transport in Semiconductors Using a Population-Dependent Many-Body Cellular Monte Carlo Approach," Journal of Heat Transfer, 139(3), pp. 032002-032002-10.
[19] Kukita, K., and Kamakura, Y., 2013, "Monte Carlo Simulation of Phonon Transport in Silicon Including a Realistic Dispersion Relation," JOURNAL OF APPLIED PHYSICS, 114(15), pp. 154312.
[20] Kukita, K., Adisusilo, I. N., and Kamakura, Y., 2014, "Monte Carlo Simulation of Diffusive-to-Ballistic Transition in Phonon Transport," Journal of Computational Electronics, 13(1), pp. 264-270.
[21] Nur Adisusilo, I., Kukita, K., and Kamakura, Y., "Analysis of Heat Conduction Property in Finfets Using Phonon Monte Carlo Simulation," pp. 17-20.
[22] Brown Iii, T. W., 2012, "A Statistical Phonon Transport Model for Thermal Transport in Crystalline Materials from the Diffuse to Ballistic Regime," Doctor of Philosophy Rochester Institute of Technology, Rochester, NY.
[23] Brown, T. W., and Hensel, E., 2012, "Statistical Phonon Transport Model for Multiscale Simulation of Thermal Transport in Silicon: Part I – Presentation of the Model," International Journal of Heat and Mass Transfer, 55(25-26), pp. 7444-7452.
[24] Brown, T. W., and Hensel, E., 2012, "Statistical Phonon Transport Model for Multiscale Simulation of Thermal Transport in Silicon: Part Ii – Model Verification and Validation," International Journal of Heat and Mass Transfer, 55(25-26), pp. 7453-7459.
[25] Gautreau, P., Chu, Y., Ragab, T., and Basaran, C., 2015, "Phonon-Phonon Scattering Rates in Single Walled Carbon Nanotubes," Computational Materials Science.
[26] Pascual-Gutierrez, J. A., 2010, "On the Theory of Phonons: A Journey from Their Origins to the Intricate Mechanisms of Their Transport," ProQuest Dissertations Publishing.
[27] Kittel, C., Introduction to Solid State Physics, 8th Edition.
[28] Shinde, S. L., and Srivastava, G. P., 2014, Length Scale Dependent Phonon Interactions, Springer Science + Business Media, New York.